THE 4th INTERNATIONAL CONFERENCE
MECHANICAL ENGINEERING IN XXI CENTURY

April 19-20, 2018
Faculty of Mechanical Engineering in Niš

Development and Implementation of Drucker-Prager Constitutive Model for Plane Strain Condition

Nikola JOVIĆ, Dragan RAKIĆ, Miroslav ŽIVKOVIĆ

Faculty of Engineering, University of Kragujevac, Sestre Janjić 6, Kragujevac
njovic1995@gmail.com, drakic@kg.ac.rs, zile@kg.ac.rs

***Abstract*—Theoretical basis of the Drucker-Prager constitutive model is given and the implicit stress integration in the case of a plane strain state is shown in this paper. The reduction of the stress and strain tensor to the plane strain case was carried out, after which an algorithm for implicit stress integration was developed using the governing parameter method. This algorithm was implemented in the PAK program package. The verification of the developed algorithm was done through several examples where the results compared with 3D model, as well as with the solutions obtained by using other software. On the basis of the obtained results it can be concluded that the developed algorithm for implicit stress integration, gives identical results with solutions using the 3D constitutive model, as well as solutions using other software.**

***Keywords*— constitutive model, implicit stress integration, plane strain, Drucker-Prager, PAK**

I. INTRODUCTION

Using the incremental theory of plasticity, the development of the algorithm for the implicit stress integration of the Drucker-Prager material model for the plane strain condition was carried out. The development of the stress tensor and the strain tensor in the case of a plane strain condition was conducted. Developed algorithm was implemented in the PAK software package. The verification of the developed algorithm was conducted through the simulation of the direct shear test as well as through the uniaxial compression test. Comparison of results obtained using the 2D finite elements with results obtained using 3D finite elements. The numerical results of the direct shear test were also compared with the experimental results.

II. ELASTIC-PLASTIC CONSTITUTIVE MATRIX

In the small strain theory, the total increment of the strain is equal to the sum of elastic and plastic strain [1], that is:

$$d\mathbf{e} = d\mathbf{e}^E + d\mathbf{e}^P \tag{1.1}$$

The stress in the material causes only the elastic part of the strain. Increase of the stress corresponding to elastic strain is determined by the following equation [2]:

$$d\boldsymbol{\sigma} = \mathbf{C}^E d\mathbf{e}^E \tag{1.2}$$

where $\mathbf{C}^E$ represents an elastic constitutive matrix.

The increase of plastic strain $d\mathbf{e}^p$ can be calculated using the yield conditions, according to which the increment of plastic strain is directly proportional to the plastic potential gradient [3], which can be written as:

$$d\mathbf{e}^p = d\lambda \frac{\partial g}{\partial \boldsymbol{\sigma}} \tag{1.3}$$

The plastic strain increment $d\mathbf{e}^p$ is normal to the surface of the plastic potential.

The scalar $d\lambda$ represents the factor of proportionality between the increase of the plastic strain and the plastic potential gradient.

By using equations (1.1) and (1.2) can be obtained by:

$$d\boldsymbol{\sigma} = \mathbf{C}^E (d\mathbf{e} - d\mathbf{e}^P) \tag{1.4}$$

In the case of a constitutive model without hardening, which is discussed in the paper, the yield surface is defined by a scalar function that depends only on the stress tensor. When a plastic strain occurs, the increment of the yield function is equal to zero, or:

$$df = \frac{\partial f^T}{\partial \boldsymbol{\sigma}} d\boldsymbol{\sigma} = 0 \tag{1.5}$$

In the case of plain strain, a differential of the yield function with respect to the stress components are:

$$\frac{\partial f^T}{\partial \boldsymbol{\sigma}} = \left[\frac{\partial f}{\partial \sigma_{xx}} \quad \frac{\partial f}{\partial \sigma_{yy}} \quad \frac{\partial f}{\partial \sigma_{xy}} \quad \frac{\partial f}{\partial \sigma_{zz}} \right] \tag{1.6}$$

where $d\boldsymbol{\sigma}$ represents the increment of the stress that can be written in vector form as:

$$d\boldsymbol{\sigma}^T = \left[d\sigma_{xx} \quad d\sigma_{yy} \quad d\sigma_{xy} \quad d\sigma_{zz} \right] \tag{1.7}$$

Using the relations (1.3) and (1.4), we get the increment of the yield function (1.5) in the following form:

$$df = \frac{\partial f^T}{\partial \boldsymbol{\sigma}} (\mathbf{C}^E d\mathbf{e} - \mathbf{C}^E d\lambda \frac{\partial g}{\partial \boldsymbol{\sigma}}) = 0 \tag{1.8}$$

where scalar $d\lambda$ can be calculated as:

$$d\lambda = \frac{\frac{\partial f^T}{\partial \boldsymbol{\sigma}} \mathbf{C}^E d\mathbf{e}}{\frac{\partial f^T}{\partial \boldsymbol{\sigma}} \mathbf{C}^E \frac{\partial g}{\partial \boldsymbol{\sigma}}} \tag{1.9}$$

Finally, using the scalar $d\lambda$ from (1.9), the increment of total stress $d\boldsymbol{\sigma}$ can be determined using the equations (1.3) and (1.4) in the function of the increment of the total strain as:

$$d\boldsymbol{\sigma} = \mathbf{C}^{EP} d\mathbf{e} \tag{1.10}$$

Where, $\mathbf{C}^{EP}$ represents elastic-plastic constitutive matrix:

$$\mathbf{C}^{EP} = (\mathbf{C}^{E} - \frac{\mathbf{C}^{E}\frac{\partial f^{T}}{\partial \boldsymbol{\sigma}}\frac{\partial g}{\partial \boldsymbol{\sigma}}\mathbf{C}^{E}}{\frac{\partial f^{T}}{\partial \boldsymbol{\sigma}}\frac{\partial g}{\partial \boldsymbol{\sigma}}\mathbf{C}^{E}}) \tag{1.11}$$

III. Stress Integration in Case of Plane-Strain Condition

In the case of the plane-strain condition, the strain tensor has the next form [4]:

$$\mathbf{e} = \begin{bmatrix} e_{xx} & e_{xy} & 0 \\ e_{yx} & e_{yy} & 0 \\ 0 & 0 & 0 \end{bmatrix} \tag{1.12}$$

Because of the symmetry of the strain tensor, it can be written using a single-index notation as:

$$\mathbf{e} = \begin{bmatrix} e_{xx} & e_{yy} & e_{xy} & 0 \end{bmatrix} \tag{1.13}$$

The stress tensor for the case of plane-strain condition has the form:

$$\boldsymbol{\sigma} = \begin{bmatrix} \sigma_{xx} & \sigma_{xy} & 0 \\ \sigma_{yx} & \sigma_{yy} & 0 \\ 0 & 0 & \sigma_{zz} \end{bmatrix} \tag{1.14}$$

or, because of the symmetry, it can be written in vector form as:

$$\boldsymbol{\sigma} = \begin{bmatrix} s_{xx} & s_{yy} & s_{xy} & s_{zz} \end{bmatrix} \tag{1.15}$$

Representation of a plane-strain is shown on Fig. 1.

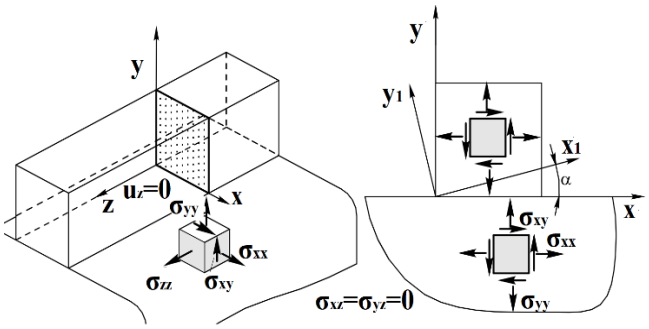

Fig. 1 Plane strain condition

Experimental material testing shows existence of a domain that defines the area of possible stress state. The surface that limits the area of possible stress area is called yield surface. In general case, the function that defines this surface depends on the stress and the material hardening and it can be represented by the following equation:

$$f = f(\boldsymbol{\sigma}, k) \tag{1.16}$$

The surface of the plastic potential is defined by the similar function as:

$$g = g(\boldsymbol{\sigma}, k) \tag{1.17}$$

The yield surfaces and the plastic potential surfaces can coincide, and then it is called associative yield condition. If they do not coincide, this is non-associative condition yield.

In the case when the stress point is inside of the yield surface, only elastic deformation will occur in the material. If the stress point reaches the yield surface, plastic strain occurs. Stress states outside this region are not possible.

The yield surface of the Drucker-Prager constitutive model in principal stress space is the cone (Fig. 2), which the main axis coincides with the hydrostatic axis [2] and it is described by the next equation:

$$f = \alpha I_1 + \sqrt{J_{2D}} - k \tag{1.18}$$

while, the plastic potential function has the following form:

$$g = \beta I_1 + \sqrt{J_{2D}} \tag{1.19}$$

In equation (1.18) and (1.19), I_1 represents the first stress invariant, J_{2D} is the second deviatoric stress invariant, while α, β, k represents material constants.

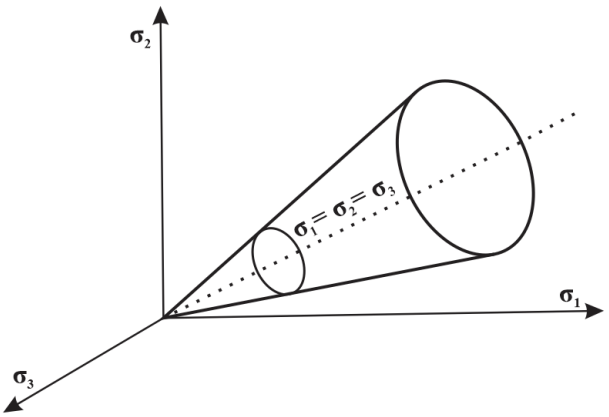

Fig. 2 The yield surface of the Drucker-Prager constitutive model

In order to determine the stress increment (1.10) it is necessary to find derivatives of the yield function and the plastic potential function with respect the stress tensor. The plastic potential function and the yield surfaces function are composite functions. By applying chain rule, these derivatives are:

$$\begin{aligned} \frac{\partial f}{\partial \boldsymbol{\sigma}} &= \frac{\partial f}{\partial I_1}\frac{\partial I_1}{\partial \boldsymbol{\sigma}} + \frac{\partial f}{\partial J_{2D}}\frac{\partial J_{2D}}{\partial \boldsymbol{\sigma}}, \\ \frac{\partial g}{\partial \boldsymbol{\sigma}} &= \frac{\partial g}{\partial I_1}\frac{\partial I_1}{\partial \boldsymbol{\sigma}} + \frac{\partial g}{\partial J_{2D}}\frac{\partial J_{2D}}{\partial \boldsymbol{\sigma}} \end{aligned} \tag{1.20}$$

IV. Implicit Stress Integration Algorithm of the Drucker-Prager Constitutive Model

In this section, the algorithm for implicit stress integration of the Drucker-Prager constitutive model in case of plane-strain state is given (TABLE I). This algorithm in presented form is implemented in the PAK program package. After algorithm implementation the verification of the algorithm was done through the numerical simulation of test examples.

V. Verification of Developed Algorithm

A. Uniaxial compression test (Oedometer Test)

The first example represents an elastic-plastic analysis of the sand specimen compression using multi-cycle uniaxial load. The axial load of the model is applied using prescribed displacement on the model top, while displacements of the model side are restricted in normal direction. Bottom of the model is fixed in all direction (Fig. 3).

Finite element model for compression test simulation consisting of one 2D finite element without midside nodes, with corresponding constraints and loads, in

accordance with the scheme in Fig. 3, is given in Fig. 4. Model dimensions are 2x2 m. Finite element model was created using software package Femap [5].

TABLE I ALGORITHM FOR IMPLICIT STRESS INTEGRATION

Known: ${}^{t+\Delta t}\mathbf{e}, {}^{t}\mathbf{e}, {}^{t}\sigma, {}^{t}\mathbf{e}^{P}$

A. Trial (elastic) solution:

$d\boldsymbol{\sigma} = \mathbf{C}^{E} d\mathbf{e}^{E} = \mathbf{C}^{E}({}^{t+\Delta t}\mathbf{e} - {}^{t}\mathbf{e})$,

${}^{t+\Delta t}\boldsymbol{\sigma} = {}^{t}\boldsymbol{\sigma} + d\boldsymbol{\sigma}, {}^{t+\Delta t}$

${}^{t+\Delta t}\mathbf{s} = {}^{t+\Delta t}\boldsymbol{\sigma} - m\,{}^{t+\Delta t}\boldsymbol{\sigma}_{m}$

Calculation of stress invariants:

$I_1 = tr(\boldsymbol{\sigma})$

$J_{2D} = \frac{1}{2}\,{}^{t+\Delta t}\mathbf{s}\,{}^{t+\Delta t}\mathbf{s}$

Yield function:

$f = \alpha I_1 + \sqrt{J_{2D}} - k$

Plastic potential function:

$g = \beta I_1 + \sqrt{J_{2D}}$

B. Check the yield condition:

IF $(f \le 0)$ trial solutions are elastic (GO TO E)

IF $(f > 0)$ elastic-plastic solutions (CONTINUE)

$\frac{\partial f}{\partial \boldsymbol{\sigma}} = \frac{\partial f}{\partial I_1}\frac{\partial I_1}{\partial \boldsymbol{\sigma}} + \frac{\partial f}{\partial J_{2D}}\frac{\partial J_{2D}}{\partial \boldsymbol{\sigma}}$

$\frac{\partial g}{\partial \boldsymbol{\sigma}} = \frac{\partial g}{\partial I_1}\frac{\partial I_1}{\partial \boldsymbol{\sigma}} + \frac{\partial g}{\partial J_{2D}}\frac{\partial J_{2D}}{\partial \boldsymbol{\sigma}}$

$d\lambda = \frac{\frac{\partial f^{T}}{\partial \boldsymbol{\sigma}}\mathbf{C}^{E} d\mathbf{e}}{\frac{\partial f^{T}}{\partial \boldsymbol{\sigma}}\mathbf{C}^{E}\frac{\partial g}{\partial \boldsymbol{\sigma}}}$

C. Correction $d\lambda$ (local iterations)

$d\mathbf{e}^{P} = d\lambda \frac{\partial g}{\partial \boldsymbol{\sigma}}$

$d\mathbf{e}^{E} = d\mathbf{e} - d\mathbf{e}^{P}$

$d\boldsymbol{\sigma} = \mathbf{C}^{E} d\mathbf{e}^{E}$

${}^{t+\Delta t}\boldsymbol{\sigma} = {}^{t}\boldsymbol{\sigma} + d\boldsymbol{\sigma}$

Calculation of new stress invariants:

$I_1 = tr(\boldsymbol{\sigma}),\ J_{2D} = \frac{1}{2}\,{}^{t+\Delta t}\mathbf{s}\,{}^{t+\Delta t}\mathbf{s}$

Yield function:

$f = \alpha I_1 + \sqrt{J_{2D}} - k$

D. IF $(ABS(f) \ge TOL)$ go back to C with new $d\lambda$

${}^{t+\Delta t}\mathbf{e}^{P} = {}^{t}\mathbf{e}^{P} + d\mathbf{e}^{P}$

E. End: ${}^{t+\Delta t}\boldsymbol{\sigma}, {}^{t+\Delta t}\mathbf{e}^{P}$

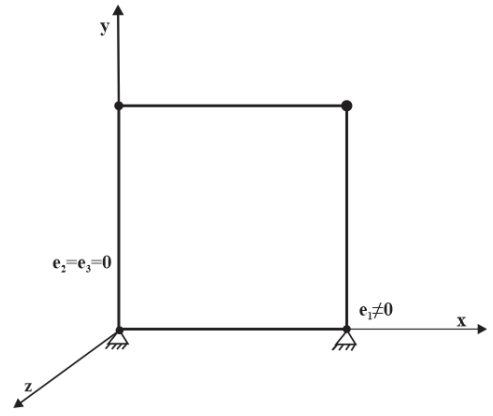

Fig. 3 Scheme of uniaxial compression test

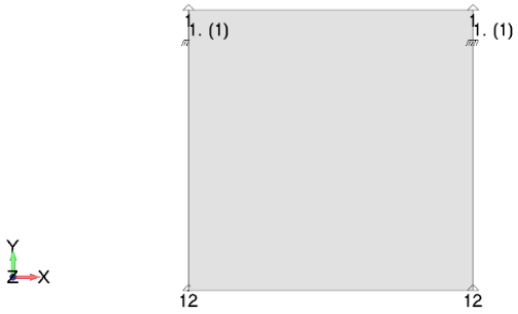

Fig. 4 Finite element model for uniaxial compression test

Material data for numerical simulation are taken from the literature [3] and they are presented in the TABLE II.

TABLE II MATERIAL PARAMETERS

Young modulus	E=100 MPa
Poison's coefficient	v=0.25
Material parameter	α=0.05
Material parameter	k=0.25 MPa

The model is loaded using load function given in Fig. 5. The displacement of the model is applied using 80 time steps. For equilibrium iterations Modified Newton method is employed.

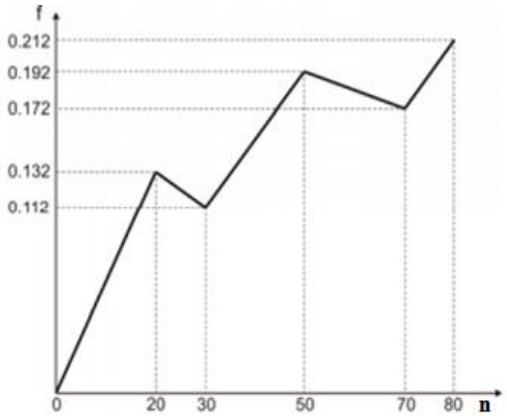

Fig. 5 Model loading function

In order to verify the developed algorithm for plane strain stress integration, a model was also created using a 3D finite element with the application of boundary conditions corresponding to a plane strain condition (Fixed translation in the direction normal to the plane of the drawing). The results of both analyses are shown in Fig. 6 and Fig. 7.

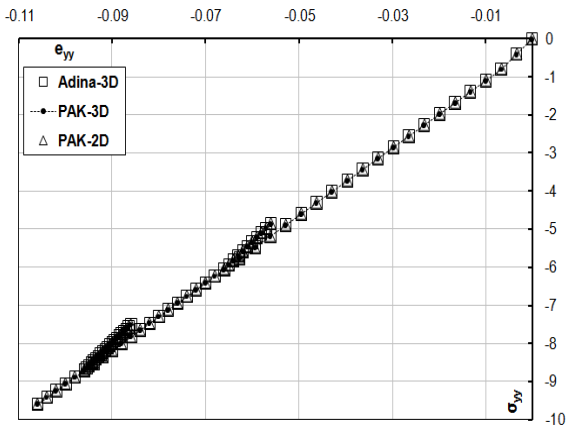

Fig. 6 Axial stress in the function of axial strain

Fig. 6 shows dependence of the vertical strain from vertical stress. Analysing the showed results, we can conclude that results of the model obtained using 2D finite elements completely coincide with the results obtained using 3D finite elements, with plane strain boundary condition.

Fig. 7 shows the dependence of the first stress invariant from the second invariant of the deviatoric stress. In the load regime, the plastic yield takes place on the Drucker-Prager yield surface, while in the unloading regime, the stress point is in the elastic area (below the failure surface-FS).

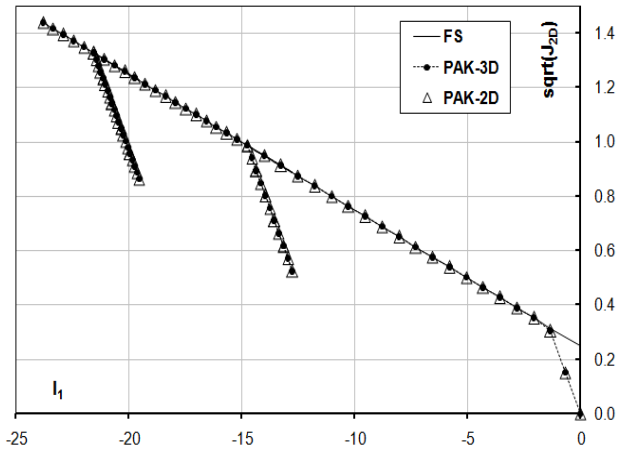

Fig. 7 Second stress invariant deviatoric function of the first stress invariant

Fig. 8 and Fig. 9 show the field of vertical displacement at the last loading step for 2D and 3D model in the plane strain condition.

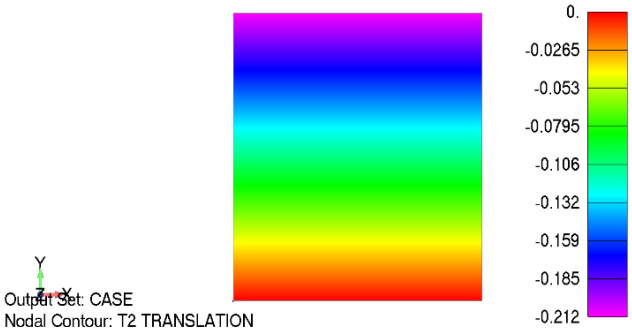

Fig. 8 The vertical displacement field in the 2D model

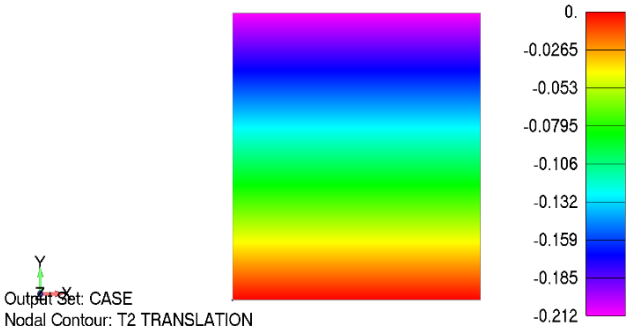

Fig. 9 Vertical displacement field for a 3D model

Based on the displacement distribution shown in Fig. 8 and Fig. 9, we can conclude that the results obtained using 2D model are identical to the results obtained using 3D model in case of plane-strain boundary condition.

B. *Direct Shear Test*

Second verification example of the developed algorithm represents numerical simulation of the direct shear test. This relatively simple test is often used to estimate constitutive model parameters. Its simulation is also suitable for constitutive model verification. Fig. 10 shows a scheme of the model for direct shear test simulation.

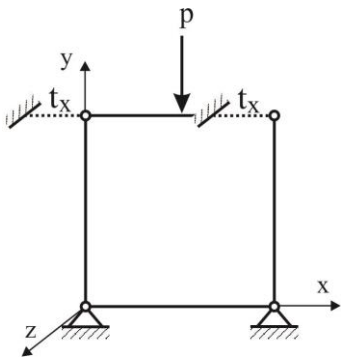

Fig. 10 Model for direct shear test simulation

Fig. 11 shows the finite element model with given boundary conditions and loads.

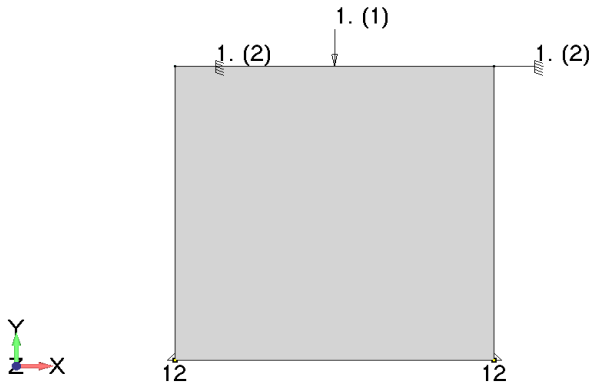

Fig. 11 Finite element model for direct shear test simulation

The bottom nodes of the model are completely constrained, and the upper nodes are free. The model load is applied in two phases. In the first phase of the load, the vertical pressure is applied to the level of stress used in the experiment. After reaching the prescribed stress, the shear load in the horizontal direction was carried out using the prescribed displacement. The model is loaded using load functions given in Fig. 12.

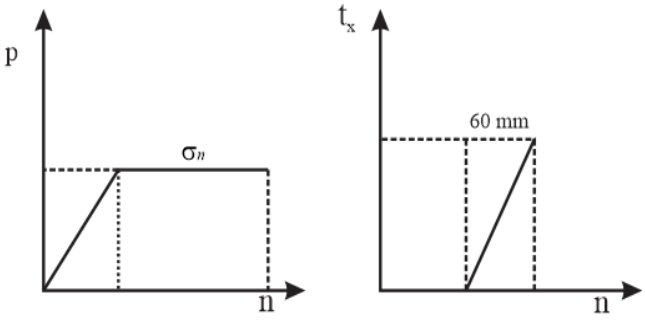

Fig. 12 Model load functions

The results of the specimen laboratory test are shown in TABLE III and represent the dependence of the shear

stress at failure of the specimen corresponding to values of the normal stress.

TABLE III MEASURED STRESS VALUES DURING FAILURE

Test No.	σ_n [kPa]	τ [kPa]
1	209	200
2	426	276
3	813	440
4	1713	927

In this example, four cases of load were analyzed. In each load case the same load functions were used, with the changed values of the normal stress given in TABLE III. Estimated material parameters of the Drucker-Prager model, using data from the TABLE III, are given in TABLE IV.

TABLE IV MATERIAL PARAMETERS

Young modulus	E=1x10^5 kPa
Poison's coefficient	v=0.3
Material parameter	α=0.1990
Material parameter	k=88.17 kPa

The results of direct shear test simulation for 2D and 3D finite elements, for the plane strain condition, in the form of displacement vs. shear stress in the horizontal are presented in Fig. 13.

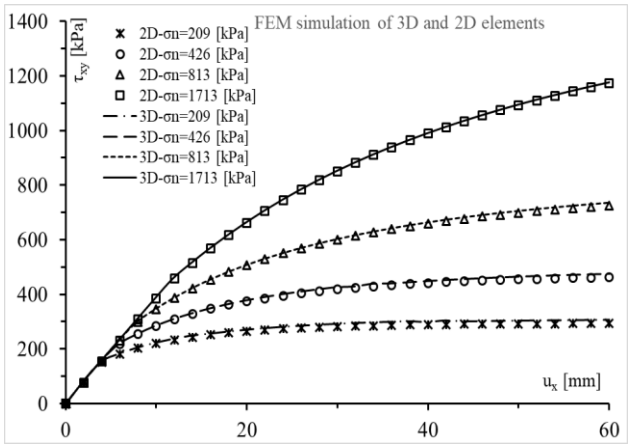

Fig. 13 Results of direct shear test simulation for case of 3D and 2D finite elements

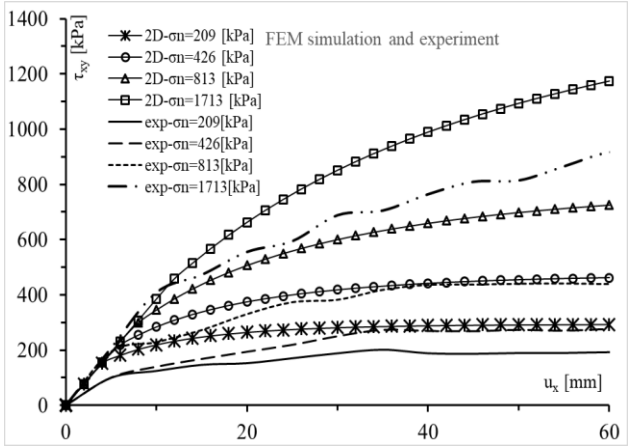

Fig. 14 The results of the experiment of the direct shear test and the simulation of the 2D model

Based on presented results, we can conclude that the results obtained using 2D finite elements are identical with the results for 3D finite elements, for the plane strain condition used.

Fig. 14 shows the comparison of the displacement vs. shear stress at used values of normal stresses obtained in numerical simulation and experimentally.

By comparing results presented in Fig. 14, we can notice that the simulation results do not match completely experimental results (the character is appropriate but the values of numerical results are higher). The reason for this deviation is the greater stiffness of the finite elements without midside nodes, used in this numerical simulation. In order to make the numerical simulation results more consistent with the experimental results, it is necessary to use finite elements with midside nodes.

Fig. 15 and Fig. 16 shows a horizontal displacement field at the last time step for 2D and 3D models respectively.

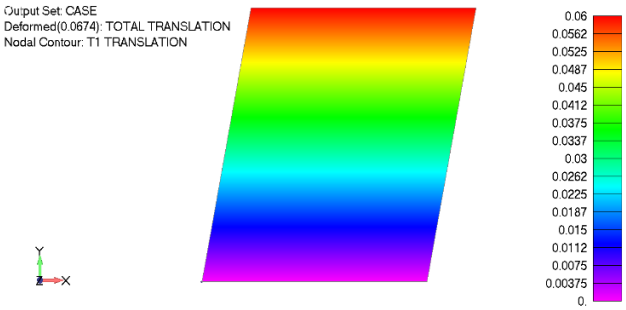

Fig. 15 Displacement field in the 2D model in horizontal direction

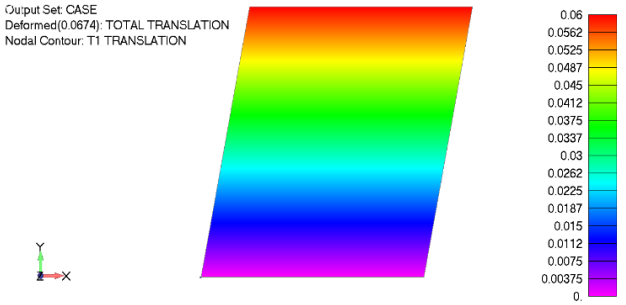

Fig. 16 Displacement field in the 3D model in horizontal direction

On the basis of the obtained displacement fields, we can notice that the results obtained by using the finite 2D elements coincide with the results of a model created by 3D elements in the plane-strain condition.

VI. CONCLUSION

The paper presents the implicit integration of the Drucker-Prager material model in the plane-strain state, using the theory of incremental plasticity. The steps of implicit stress integration of this material model are presented in the form of the algorithm which is implemented in the PAK program package. The developed algorithm was verified using uniaxial compression test and direct shear test. The material parameters of the Drucker-Prager constitutive model were obtained by estimation based on experimental results. The results of numerical simulations for 2D finite elements are compared with results obtained using 3D finite elements for plane strain condition. An analysis of the numerical simulation results indicates that the results

obtained by the 2D finite elements completely coincide with the results obtained by using 3D finite elements in the same condition. Simulation results of the direct shear test do not match experimental results values due to greater stiffness of the finite elements without midside nodes which are used in the simulation.

Further development of the PAK software package in the field of computational geomechanics will be development of the integration algorithms for the plane-strain condition of other constitutive models for application in field of geomechanics.

ACKNOWLEDGEMENTS

The authors gratefully acknowledge partial support by Ministry of Science and Technology of the Republic of Serbia, grants TR37013 and TR32036.

REFERENCES

[1] M. Kojic, "A General Concept of Implicit Integration of Constitutive Relations for Inelastic Material Deformation", Kragujevac: Center for Scientific Research SANU and University of Kragujevac, 1993.

[2] D. Rakić, "Numeričko rešavanje geomehaničkih problema primenom Draker-Prager materijalnog modela", Magistarska teza, Kragujevac: Univerzitet u Kragujevcu, Mašinski fakultet, Srbija, 2009.

[3] D. Rakic, "Razvoj i primena materijalnih modela u statičkoj i dinamičkoj analizi nasutih brana", Doktorska disertacija, Kragujevac: Fakultet inzenjerskih nauka Univerziteta u Kragujevcu, 2014.

[4] М. Којић, "Метод коначних елемената 1- Линеарна анализа", Крагујевац: Универзитет у Крагујевцу, Машински факултет, 2010.

[5] Siemens, "Femap - Finite Element Modeling and Post Processing Application", FEMAP v11.3.2, 2015.